Conformational Study in Water by NMR and Molecular Modeling of Cyclic Glutamic Acid Analogues as Probes of Vitamin K Dependent Carboxylase

Valéry Larue,[†] Josyane Gharbi-Benarous,[†,‡] Francine Archer,[†] Robert Azerad,[†] and Jean-Pierre Girault*,[†]

Université René Descartes-Paris V, Laboratoire de Chimie et Biochimie Pharmacologiques et Toxicologiques (URA 400 CNRS), 45 rue des Saint-Pères, 75270 Paris Cedex 06, France, and Université Denis Diderot-Paris VII, UFR Chimie, 2 Place Jussieu, F-75251 Paris Cedex 05, France

Received October 10, 1995[⊗]

The conformational analysis of four glutamic acid analogues containing a cyclopentyl or cyclohexyl ring, substituted in position 1 by a BOC protected amino group and a methyl ester group and in position 3 by a free carboxylate group, has been carried out in an aqueous environment, by ^{1}H and ^{13}C NMR spectroscopy, and molecular dynamics (MD). Their structural properties were under investigation for a structure−activity relationship analysis to determine the preferred conformation in the carboxylase active site. For each compounds, resulting conformations from NMR and MD data were analyzed and classified according to the dihedral angles $\chi 1$ and $\chi 2$, the distances and the spatial distribution involving charged or substituted C- and N-terminal groups. A reduced number of conformational families were found to be in qualitative agreement with NMR and MD data. A comparison between these different classes of the active and nonactive derivatives was achieved.

A liver microsomal carboxylase is responsible for the vitamin K-dependent conversion of selected glutamic acid residues of precursor proteins to γ-carboxyglutamic acid (Gla) residues of several plasma clotting factors[1−3] (the historical aspects of vitamin K action have been adequately reviewed[4]) (Figure 1). Using relatively simple substrate analogues such as the tripeptides BOC-Glu-Glu-Val corresponding to the *N*-terminal sequence of descarboxyprothrombin or shorter substrates, BOC-Glu-OMe, it was demonstrated that the decarboxylation reaction occurred.[5−9] These low-affinity peptides have proven to be useful for demonstrating several aspects of the mechanistic features of the reaction.[5−12]

In the search for more efficient carboxylase inhibitors, it was necessary to rationalize structurally-related affinities, that might result from privileged interactions of the side chain carboxylate group with the carboxylase active site and possibly to determine the conformation of the Glu side chain in the inhibitor-carboxylase complex. The cyclic glutamic acid analogues BOC-X-OMe where X was conformationally restricted glutamic acid analogues **1**−**5** (Figure 2), such as the cyclo derivatives, 1-amino-1,3-dicarboxycyclohexane or -cyclopentane (*cis* or *trans*), were tested[13] with the intention of directing the carboxylic group of the side chain in a definite position, allowing a three-dimensional exploration of the binding site of the carboxylase[5−9] (Table 1). We report here a NMR and MD study in aqueous solution, for the *cis*- and *trans*-1-[(*tert*-butyloxycarbonyl)amino]cyclohexane(or cyclopentane)-3-carboxylic acid 1-methyl ester, hereafter named respectively, BOC-*cis*-C6-OMe **6** and *trans*-**7**, BOC-*cis*-C5-OMe **8** and *trans*-**9** (Figure 2), in order to understand their structure−activity relationship in evaluating the spatial position of the γ-carboxylate of the side chain relative to the peptide chain.

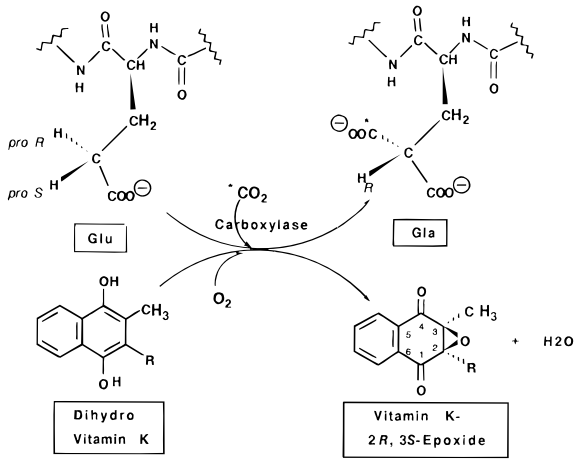

Figure 1. The liver microsomal vitamin K-dependent carboxylase. The enzymatic carboxylation reaction is coupled to the oxidation of the reduced hydronaphtoquinone form of the vitamin to the vitamin K-2*S*,3*R*-(+)-epoxide. The 3-position is occupied by a phytyl group in phylloquinone and by an unsaturated polyisoprenyl group of varying length in the bacterially synthesized menaquinones. The stereochemistry of the reaction has now been solved and the γ-*pro-S* hydrogen of the glutamyl residue is removed followed by inversion of configuration during CO_2 addition.

RESULTS AND DISCUSSION

Conformational Analysis. These derivatives display some flexibility. In cyclopentane the angle of maximum puckering rotates without substantial change in potential energy. However, the presence of the three substituents will give rise to an induced potential energy barrier opposing free pseudorotation. The consequence of "limited" pseudorotation and a description of conformations was developed. In the present article, we propose an accurate description of rings in cyclohexyl and cyclopentyl analogues and the correlated conformations of the C(3)−(γ)CO_2H side chain. The methodology presented illustrates the usefulness of molecular modeling in elucidating possible solution confor-

[†] Université René Descartes-Paris V.
[‡] Université Denis Diderot-Paris VII.
[⊗] Abstract published in *Advance ACS Abstracts,* April 15, 1996.

S0095-2338(95)00153-3 CCC: $12.00

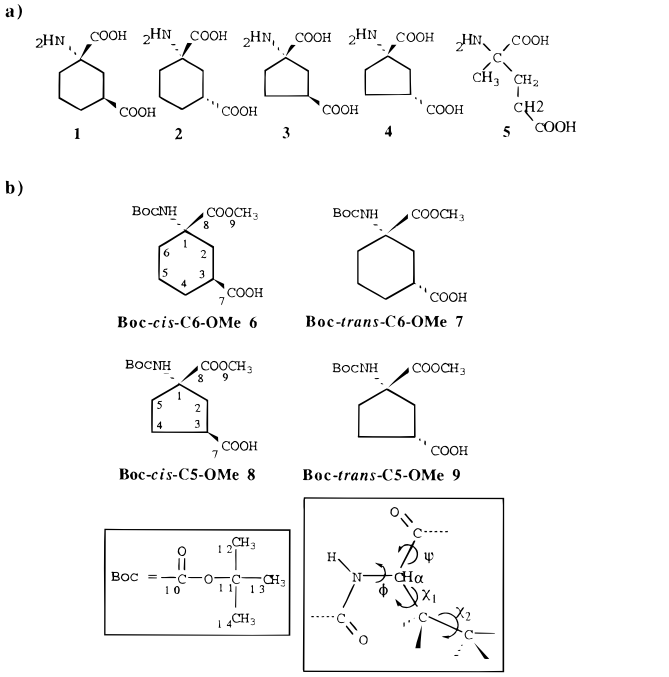

Figure 2. (a) Structures of α-substituted and cyclic glutamic acid analogues **1**−**5**. (b) Structures of cyclohexane and cyclopentane-derived analogues of glutamic acid: *cis*- and *trans*-1-[(*tert*-butyloxycarbonyl)amino]cyclohexane (or cyclopentane)-3-carboxylic acid-1-methyl ester, named respectively, BOC-*cis*-**6** and *trans*-C6-OMe **7**, BOC-*cis*-**8**, and *trans*-C5-OMe **9**.

Table 1. Carboxylation of the Tripeptides Boc-X-Glu-Val or the Derivatives Boc-X-OMe (X = Glutamic Acid Analogues)

BocX-Glu-Val or BocX-OMe	K_m (mM)	K_i (mM)	V_{max} nM CO_2 incorporated mn^{-1} (mg protein)$^{-1}$
Boc-Glu-Glu-Val	1.7 ± 0.2		0.93 ± 0.01
Boc-(DL)-2Me-Glu-Glu-Val	18.5 ± 3.5		0.50 ± 0.04
Boc-(DL)-*cis*-C6-Glu-Val	15.5 ± 1.5		0.80 ± 0.10
Boc-(DL)-*trans*-C6-Glu-Val	7.0 ± 1.9		0.35 ± 0.05
Boc-(DL)-*cis*-C5-Glu-Val	12.2 ± 0.8		0.80 ± 0.08
Boc-(DL)-*trans*-C5-Glu-Val	4.4 ± 0.0		0.40 ± 0.05
Boc-Glu-OMe	5.5 ± 0.5		0.34 ± 0.01
Boc-(DL)-2Me-Glu-OMe		>60[b]	
Boc-(dl)-*cis*-C6-OMe		65[b]	
Boc-(dl)-*trans*-C6-OMe		45[b]	
Boc-(dl)-*cis*-C5-OMe		40[b]	
Boc-(dl)-*trans*-C5-OMe		20[b]	

[a] Competitive inhibition relative to the substrate Boc-Glu-Glu-Val. [b] Competitive inhibition relative to the substrate Boc-Gln-OMe.

mations and to explore fully the conformational space of these compounds and NMR data in revealing that approximate solution structures can be estimated. NMR parameters reflect the virtual conformation and at the same time the structural information of the different conformations generated by MD are of great benefit in predicting the conformation in solution. The different biological activity observed in the formation of an inhibitor-carboxylase complex could be due to structural difference, localized flexibility, minor conformers, or a particular transition state implied in reaction with the receptor.

The preferred conformer of cyclohexane is the *chair* form in which all dihedral angles have an absolute value close to 56°. In this conformation all bonds (endocyclic as well as exocyclic) are staggered thus explaining the minimum in conformational strain. The energy barrier to convert a *chair* form into another one is close to 10−12 kcal mol^{-1}; this *chair*−*chair* conversion is a complex process of cycle inversion.[14] The *chair* form of cyclohexane is considered "rigid" since it must undergo cycle inversion of relatively high energy to yield other conformers. However besides the rigid *chair* conformers, cyclohexane also exists as flexible forms which include the *boat* conformer and the *twist* form. The *boat* and *twist* forms represent the local energy maxima with the former about 5−6 kcal mol^{-1}, above the global minimum of the *chair* forms. The *boat* and the *chair* forms show only equatorial and axial substituents positions.

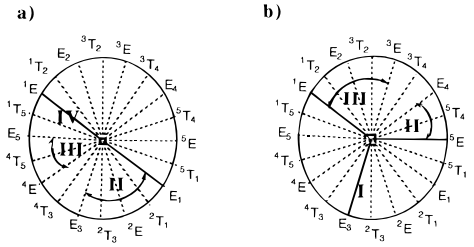

Figure 3. Pseudorotational pathway of cyclopentane ring for (a) Boc-*cis*-C5-OMe **8** and (b) Boc-*trans*-C5-OMe **9**. Each exterminal point of dotted radials in the circle represents a specific **E** form or **T** conformations. Heavy arrows indicate the corresponding family type.

In cyclopentane the bond angles have values close to the optimum; therefore, the strain in the molecule arises essentially from bond opposition and is partly relieved by puckered conformations. In the two flexible forms, *envelope* **E** and *halfhchair* **T** conformers, the following types of exocyclic bonds have been recognized: *equatorial*, *axial*, and *isoclinal* or *bisectional* bonds for ring substituent positions. The two conformers E and T are extremes of symmetry in the pseudorotational circuit of cyclopentane: 10 envelope and 10 half-chair forms interconvert by this process (Figure 3). The pseudorotation circuit of cyclopentane is essentially of constant strain without substituent; in contrast the trisubstituted cyclopentanes **8** and **9** present maxima and minima with the less stable conformer about 4 kcal mol^{-1} above the global minimum.[14−17]

The final structures obtained after several mechanics molecular calculations were examined for the overall energetic favorability and compared with the structure derived from the NMR data. The torsion angles of generated structures can be correlated to the corresponding coupling constants by using Karplus-type equations.[18−20]

NMR Spectroscopy. For the four derivatives, only one set of proton and carbon resonances was observed, except for the N-BOC and ester chain which indicates that slow conformational change occurs for these two parts of side chains. For the cyclic residue, a unique set of resonance lines was found for each atom. This could result from an averaging of chemical shifts and coupling constants due to fast conformational changes.

The conformational analysis is based on the vicinal $^3J_{^1H,^1H}$ and $^3J_{^{13}C,^1H}$ coupling constants reported in Table 2. Determination of heteronuclear $^{13}C,^1H$ coupling constants by the selective 2D INEPT experiment[21] is especially helpful for 3-H bonds in order to determine the relative positions of the substituents on the C5-ring. The vicinal coupling constants were obtained from these spectra by iterative techniques on a spectral simulation (PANIC).

The BOC-*cis*-C6-OMe **6** always adopts the chair conformation C1 with γ-CO_2^- equatorial and the minimal sterical

Table 2. ^{1}H, ^{1}H and ^{1}H, ^{13}C Coupling Constants in D_2O (Hz, Error 0.5 Hz) Values Confirmed by Simulation of the Signals (Program PANIC)[a]

J/Hz		**6**	**7**	**8**	**9**
^2J	2a,2b	−12.5	−12.7	−13.5	−13.5
	4a,4b	−12.5	−12.8	−12	−12
	5a,5b	−12.5	−13	−12	−12
	6a,6b	−12.7	−12.9		
^3J	3,2a	12.8	3.8	7.5	7
	3,2b	3.5	10.8	8	10
	3,4a	12.8	3.8	7.5	9
	3,4b	3.2	10.3	9	8
	4a,5a	3.5	4.0	9.5	9
	4a,5b	12.5	4.5	6	7
	4b,5a	3.4	11	5	7
	4b,5b	3.2	4.0	8	8
	5a,6a	3.4	4.0		
	5a,6b	3.5	11		
	5b,6a	12.7	4.0		
	5b,6b	3.5	4.0		
^3J	3-H,1-C			<1	<1
	3-H,5-C			<1	<1

[a] The **a** face of the cyclohexane or cyclopentane ring is that which contains the carboxyl group in position 1; 3-H noted **a** (for *trans*-isomers) or **b** (for *cis*-isomers) according to the geometrical isomerism of the proton (H**a** and NH_3^+ *trans*; H**b** and NH_3^+ *cis*).

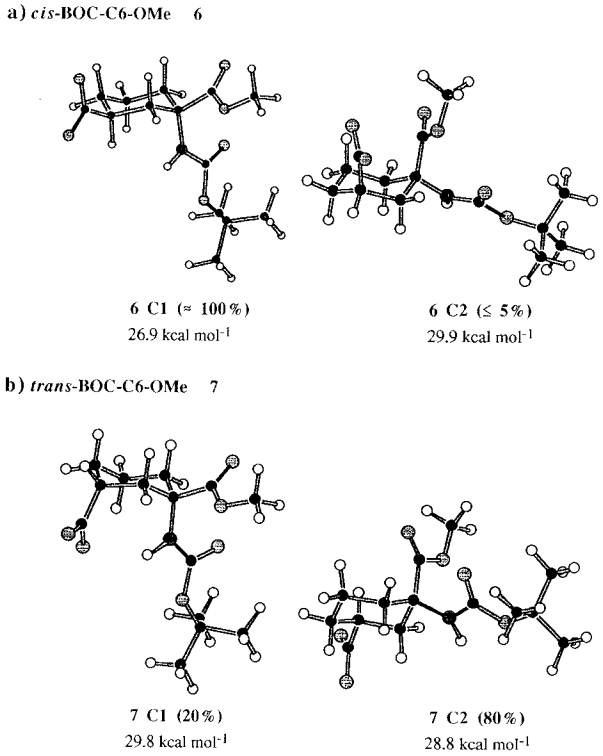

Figure 4. Stable structures generated by MD with a selected value of the relative permittivity ($\epsilon = 5$) or with water molecules and their energies, (a) for Boc-*cis*-C6-OMe **6** and (b) for Boc-*trans*-C6-OMe **7** at neutral pH. In parentheses, their percentage in solution deduced from NMR data. The **C1** conformer corresponds to the chair conformation of the cyclohexane ring with the bulky group BOC-NH axial; in the **C2** conformer BOC-NH is equatorial.

hindrance represented in Figure 4a. Using the extreme values of $^3J_{ax,ax} = 12.0$ Hz and $^3J_{eq,eq} = 3.0$ Hz it is possible to estimate the molecular ratio "*x*" of conformer C1:

$$J_{obs} = x(^3J_{ax,ax}) + (1 - x)(^3J_{eq,eq})$$

So, $J_{obs} = 12.8$ Hz → ≈100% of conformation C1.

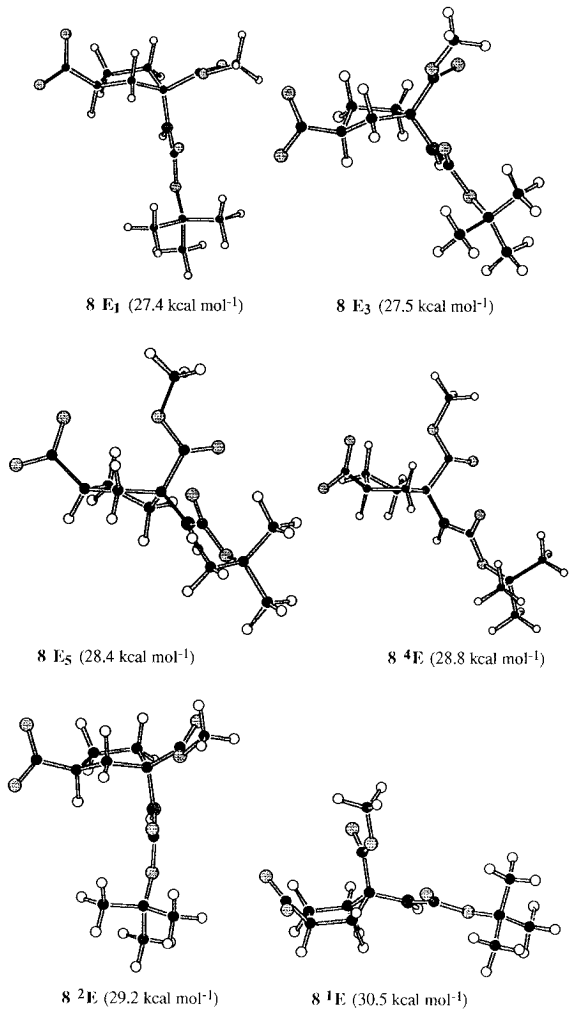

Figure 5. Achieved conformations for BOC-*cis*-C5-OMe **8** at neutral pH by MD with water molecules and in parentheses, the energies of the corresponding C5 molecules, minimized by a single iteration of the steepest descent algorithm, after removing water molecules. The experimental NMR values are not in good agreement only with those calculated for conformation **^{1}E**.

The coupling constants of BOC-*trans*-C6-OMe **7** are averaged: the C2 conformer (γ-CO_2^- equatorial) is predominant but in conformational equilibrium with the C1 conformer (γ-CO_2^- axial) being very likely stabilized by an electrostatic interaction between the 1-amino-BOC and the 3-carboxylate [Figure 4b]. $J_{obs} = 10.8$ Hz, $x \approx 0.8$ → 80% of conformation C2.

The BOC-*cis*-C5-OMe **8** will adopt a predominant conformation with the minimal steric hindrance due to the two isoclinal or equatorial 1,3-groups (1-NHBOC, 3-carboxylate or 1-methyl ester, 3-carboxylate) (Figure 5). The measurement of heteronuclear long-range $^3J_{^{13}C-^1H}$ coupling constants (Table 2) are in good agreement with the calculated values (Table 4) for conformations **8 E_1**, **8 ^{2}E**, **8 E_3**, **8 ^{4}E** or **8 E_5** (Figure 5) but are not in good agreement with the calculated values for conformation ^{1}E.

The isomer BOC-*trans*-C5-OMe **9** may be found as a mixture of the two sterically favored conformations: one with γ-CO_2^- group equatorial and another one where the γ-CO_2^- group is less equatorial on C-3. Our observed values include a large participation of conformers **9 ^{1}E**, **9 E_2**, **9 ^{3}E**, **9 E_4** or **9 ^{5}E** (Figure 6), but the experimental values of compound **9** are not in good agreement with the calculated values (Table 5) for conformation E_3.

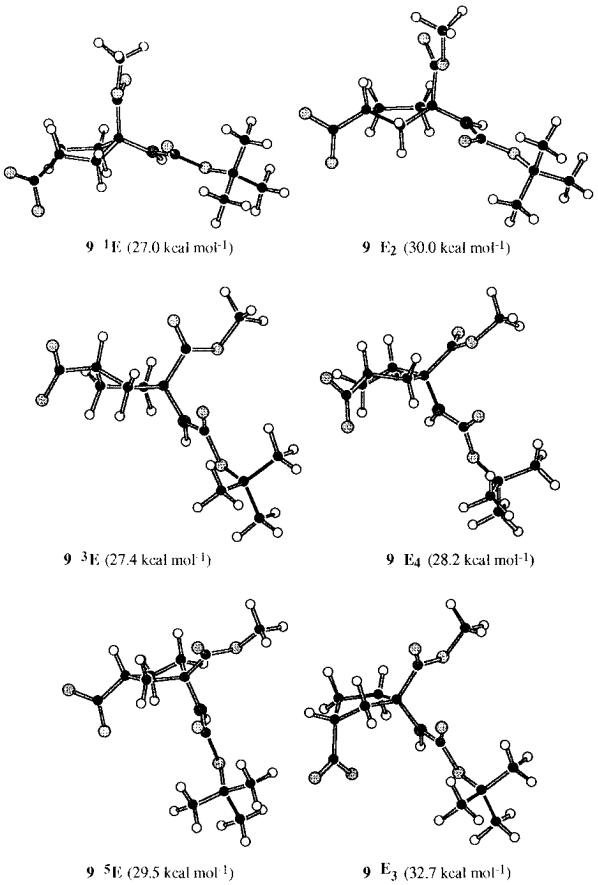

Figure 6. Achieved conformations for Boc-*trans*-C5-OMe **9** at neutral pH by MD with water molecules and only the forms, *envelope* **E** are represented; in parentheses, the energies of the corresponding C5 molecules, minimized by a single iteration of the steepest descent algorithm, after removing water molecules. The experimental NMR values are not in good agreement only with those calculated for conformation $\mathbf{E_3}$.

Molecular Modeling. We performed computational chemical methods (molecular dynamics and molecular mechanics calculations), starting with the X-ray crystal structures[22,23] of the *cis*-C6 **1** and *trans*-C5 **4** for the simulation of **6**, **7** and **8**, **9** respectively. Charges and atomic potentials were then redefined for the new molecules (**6**−**9**) using the built-in algorithm of the program. The structures were minimized, "steepest descent" and "conjugate gradients" steps, until convergence. Electrostatic interactions are calculated in the force field[24] by a coulombic expression. The final structures obtained after several such calculations were examined for the overall energetic favorability and compared with the structure derived from the NMR data.

A good procedure for choosing the appropriate force field to identify the experimentally determined conformation as the lowest energy structure is to fit the parameters of the interaction function to results (potential or field) of ab initio quantum calculations on small molecular cluster. However the alternative is to fit the force field parameters to experimental data like in our case, NMR data. The choice of a particular force field should depend on the type of system for which it has been designed.

In order to develop an adequate molecular model of the four analogs, in a first time, we have tested the ability of two force fields, Tripos and CVFF, to reproduce the experimental, NMR-determined conformations of the **7** compound which is in a "rigid" *chair*−*chair* conformational equilibrium (80:20). The lowest energy conformation found with the CVFF force field using $\epsilon_r = \mathbf{5}$ was in excellent agreement with the experimental structure. This result has suggested us that the Biosym CVFF force field was an adequate tool for modeling the **7** compound, and it shall be utilized in molecular modeling studies of the other three structural analogs. We used the CVFF force field from Dauber−Osguthorpe in which cross-terms represent the coupling of the deformations of internal coordinates and describe the coupling between adjacent bonds. These terms are required to reproduce accurately experimental vibrational frequencies and therefore the dynamic properties of molecules. A Morse function was used to describe the stretching of bonds.

Table 3. Energy, Torsion Angles, and Calculated[a] Coupling Constants (^3J Hz) Computed for **6** and **7**, from the Different Conformations Generated by MD at Neutral pH[c]

		Boc-*cis*-C6-OMe **6**		Boc-*trans*-C6-OMe **7**	
		C_1	C_2	C_1	C_2
E_p/kcal mol^{-1}		26.9[b]	29.9[b]	29.8[b]	28.8[b]
ϕ (deg) (^{J}/Hz)	3,2*ax*	−174.8	43.2	−41.8	−176.2
		(12.3)	(5.7)	(5.8)	(12.3)
	3,2*eq*	−60.4	−68.4	70.5	−62.1
		(3.0)	(2.4)	(2.2)	(3.1)
	3,4*ax*	173.8	−41.7	41.2	173.9
		(12.2)	(5.8)	(6.0)	(12.2)
	3,4*eq*	57.4	72.8	−73.3	57.5
		(3.6)	(2.0)	(2.0)	(3.6)
	4*ax*,5*ax*	−169.9	169.4	−169.4	−169.0
		(12.0)	(12.0)	(12.0)	(12.0)
	4*ax*,5*eq*	−53.1	53.2	−53.2	−53.0
		(4.2)	(4.2)	(4.1)	(4.2)
	4e,5*ax*	−54.3	54.8	−55.0	−53.5
		(4.1)	(3.9)	(3.9)	(4.2)
	4e,5*eq*	62.0	−61.5	61.2	62.5
		(3.1)	(3.1)	(3.2)	(2.9)
	5*ax*,6*ax*	172.2	−171.9	172.0	170.7
		(12.2)	(12.2)	(12.2)	(12)
	5*ax*,6*eq*	58.5	−58.3	58.4	57
		(3.5)	(3.4)	(3.4)	(3.7)
	5e,6*ax*	55.9	−55.7	55.9	54.7
		(3.8)	(3.8)	(3.8)	(4.1)
	5*eq*,6*eq*	−57.7	57.9	−57.7	−59.0
		(3.5)	(3.5)	(3.5)	(3.4)

[a] The coupling constants values $^3J_{HH}$ would be calculated using Karplus-type equations.[18−20] [b] Potential energies of the structures generated by a protocol with a selected value of the relative permittivity ($\epsilon = 5$). [c] The **a** face of the cyclohexane ring is that which contains the carboxyl group in position 1; H noted *ax* or *eq* according to the geometrical isomerism of the proton (H*ax* axial; H*eq* equatorial).

A widely used method to mimic the solvent screening effect is to use a distance-dependent relative permittivity $\epsilon = r$, leading to an r^2 dependence of the coulombic energy.[25] In a previous study,[22] these experiments with $\epsilon = r$, allowed us to confirm some of the results obtained by NMR spectroscopy, but the force field seemed unsuitable to characterize the 1,3-diaxial electrostatic interactions and thus had to be modified. Use of a distance-dependent dielectric constant ($\epsilon = r$) in the absence of explicit solvent is common, but it is a crude approximation to reality and cannot deal properly with strong charge interactions such as occur in these molecules. Hence the behavior of the calculations under this protocol was not unexpected. It is possible explicitly to model the solvent effect in the vicinity of the molecules: we used the electrostatic interaction expression $E = K \times q_1 q_2/\epsilon r$ and tried to adjust the relative permittivity to a value, between 1 and 78.5,[25] corresponding to the

Table 4. Energy, Torsion Angles, and Calculated[a] Coupling Constants (^3J Hz) Computed for **8**, from Different Conformations Generated by MD at Different Protonation States[a]

		Boc-*cis*-C5-OMe **8**					
		E$_1$	E$_3$	E$_5$	^{4}E	^{2}E	^{1}E
E_p/kcal mol^{-1}		27.4[b]	27.5[b]	28.4[b]	28.8[b]		
		29.7	30.1[c]	29.2[c]	29.7[c]	29.3[c]	30.8[c]
ϕ (deg) (^3J/Hz)	3b,2a	−161.9	−167.9	−125.5	−151.7	−171.4	−94.6
		(11.9)	(7.7)	(3.3)	(6.5)	(7.9)	(1.3)
	3b,2b	−44.5	−51.9	−10.8	−36.9	−53.7	−26.9
		(6.5)	(5.0)	(10.0)	(7.2)	(4.7)	(8.5)
	3b,4a	135.8	172.4	156.6	169.5	149.8	130.4
		(7.2)	(7.9)	(6.8)	(7.8)	(6.1)	(3.8)
	3b,4b	16.4	51.4	35.8	48.2	30.6	11.4
		(10.7)	(5.1)	(7.4)	(5.6)	(8.0)	(9.9)
	4a,5a	−21.9	−38.5	−46.1	−46.2	8	−33.5
		(10.2)	(7.0)	(5.9)	(5.8)	(10.0)	(7.6)
	4a,5b	−94.1	−152.7	−163.8	−162.3	−106.7	−151.1
		(0.4)	(6.5)	(7.5)	(7.4)	(1.7)	(6.4)
	4b,5a	139.6	91.2	73.6	74.4	125.2	84
		(8.1)	(1.3)	(2.3)	(2.2)	(3.3)	(1.6)
	4b,5b	23.7	−33	−44.1	−41.8	10.5	−33.6
		(10.0)	(7.8)	(6.2)	(6.5)	(10.0)	(7.6)
	3b-H,1-C	79.8	72.8	109.5	86.4	72.9	139.6
		(0.6)	(0.8)	(1.3)	(0.5)	(0.8)	(4.2)
	3b-H,5-C	−103.5	−69.5	−85.4	−72.2	−92.4	−110.4
		(0.9)	(1.0)	(0.5)	(0.8)	(0.5)	(1.4)

[a] The coupling constants values $^3J_{HH}$ and $^3J_{CH}$ would be calculated using Karplus-type equations.[18−20] [b] Potential energies of the structures generated by a protocol with a selected value of the relative permittivity ($\epsilon = 5$). [c] Potential energies of the structures generated by a protocol in a solvation box. The molecules are minimized by a single iteration of the steepest descent algorithm, after removing water molecules. [d] The **a** face of the cyclopentane ring is that which contains the carboxyl group in position 1; H noted **a** or **b** according to the geometrical isomerism of the proton (H**a** and NH_3^+ *trans*; H**b** and NH_3^+ *cis*).

Table 5. Energy, Torsion Angles, and Calculated Coupling Constants[a] (^3J Hz) Computed for **9**, from Different Conformations Generated by MD[d]

		Boc-*trans*-C$_5$-OMe **9**					
		^{1}E	E$_4$	^{5}E	E$_2$	^{3}E	E$_3$
E_p/kcal mol^{-1}		27.0[b]	28.3[b]	28.4[b]		28.4[b]	30.7[b]
		29.3[c]	30.5[c]	30.1[c]	30.1[c]	30.4[c]	
ϕ (deg) (^3J/Hz)	3a,2a	43.5	47.1	14.9	52.7	56.2	−32.6
		(6.5)	(5.5)	(9.7)	(4.9)	(4.4)	(7.7)
	3a,2b	160.9	161.6	129.2	171.3	173.4	81.8
		(11.5)	(11.9)	(3.8)	(7.8)	(7.9)	(1.4)
	3a,4a	−13.9	−52.4	37.6	−32.1	−50.6	33.9
		(11.2)	(4.3)	(7.1)	(7.7)	(5.2)	(7.6)
	3a,4b	−133.3	−173.5	−158.7	−150.9	−171	−85
		(6.0)	(12.8)	(7.1)	(6.3)	(7.8)	(1.5)
	4a,5a	−26.6	41.8	44.5	−8.2	27	−32.9
		(9.5)	(6.6)	(6.1)	(10.0)	(8.5)	(7.7)
	4a,5b	−142.7	−73.8	−73.2	−123.3	−87.3	−147
		(8.6)	(1.2)	(2.3)	(3.1)	(1.4)	(5.9)
	4b,5a	91.2	163	164.5	109.5	146.4	85.4
		(0.4)	(12.2)	(7.5)	(1.9)	(5.8)	(1.5)
	4b,5b	−24.9	47.4	46.9	−5.6	32.1	−28.8
		(9.8)	(5.5)	(5.7)	(10.1)	(7.9)	(8.3)
	3a-H,1-C	−80.6	−78	−106.1	−70.7	−67.4	−151.4
		(0.5)	(0.6)	(1.0)	(0.9)	(1.1)	(5.4)
	3b-H,5-C	105.8	67.9	83.5	90.2	71.2	151.6
		(1.1)	(1.1)	(0.5)	(0.5)	(0.9)	(5.4)

[a] The coupling constants values $^3J_{HH}$ and $^3J_{CH}$ would be calculated using Karplus-type equations.[18−20] [b] Potential energies of the structures generated by the protocol with a selected value of the relative permittivity ($\epsilon = 5$). [c] Potential energies of the structures generated by the protocol in a solvation box. The molecules are minimized by a single iteration of the steepest descent algorithm, after removing water molecules. [d] The **a** face of the cyclopentane ring is that which contains the carboxyl group in position 1; H noted **a** or **b** according to the geometrical isomerism of the proton (H**a** and NH_3^+ *trans*; H**b** and NH_3^+ *cis*).

interactions in aqueous solution. We have used the results of the NMR experiments on the conformational equilibrium observed for the *trans*-1-aminocyclohexane-1,3-dicarboxylic acid (*trans*-C6) at pH 4.0 and 7.0. We have run dynamics starting from each one of the possible chairs for this isomer, with different values of ϵ and correct energy differences between the two chairs forms are obtained for $\epsilon = 5$. With this value of the relative permittivity, experiments are run starting from each of the possible conformers for the two isomers.

It seemed better to mimic the solvent with explicit modeling of water. Since interactions occur between the

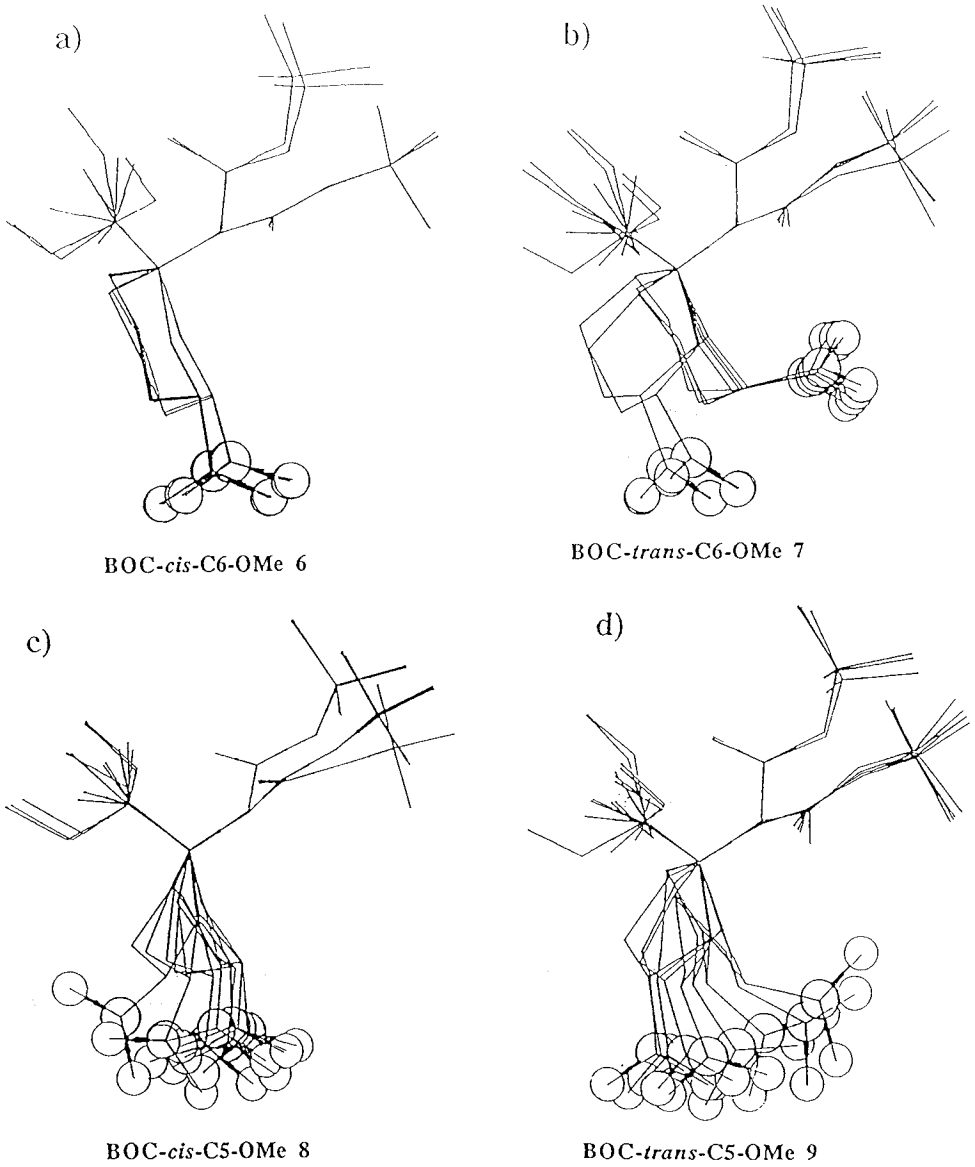

Figure 7. Conformational averaging for the four cyclohexane and cyclopentane-derived analogues of glutamic acid in solution at pH 7: (a) superposition of energy minimized structures for Boc-*cis*-C6-OMe **6 C1**; (b) superposition of energy minimized structures for Boc-*trans*-C6-OMe **7 C1** and **7 C2**; (c) superposition of energy minimized structures for Boc-*cis*-C5-OMe **8** ($\mathbf{E}_1$, $^2\mathbf{E}$, $\mathbf{E}_3$, $^4\mathbf{E}$, $\mathbf{E}_5$); and (d) superposition of energy minimized structures for Boc-*trans*-C5-OMe **9** ($^1\mathbf{E}$, $\mathbf{E}_2$, $^3\mathbf{E}$, $\mathbf{E}_4$, $^5\mathbf{E}$). Hydrogens have been removed for clarity.

solvent and backbone charged groups, we have constructed solvation boxes around the charged end-groups of the molecules containing several water molecules using periodic boundary conditions. A cut-off function of 11 Å was applied for nonbonded interactions. The relative permittivity was set to $\epsilon = 1$, and a box contained 48 (12−12−12) water molecules. However, it is not of practical use: the CPU times are much longer than for a single molecule, and the energies obtained are those of BOC-C5-OMe + 48 H_2O systems; thus the energies of the minimized C5 molecules themselves are very different to evaluate.

In the case of the cyclopentane isomers **8** and **9**, we have carried simulation of these molecules in aqueous environment to get the best agreement between theoretical (MD) and experimental (NMR) data. A protocol is used with explicit solvent molecules incorporated during the run. Then, when a good agreement is obtained, nothing else was changed in the force field considering that it was well-fitted.

Molecular Mechanics. The different conformations of the (**6**−**9**) isomers are minimized by molecular mechanics. All calculations are performed, using a relative permittivity (dielectric constant) with considered values of ϵ, $1 \leq \epsilon \leq 5$, $\epsilon = 4r$ and $\epsilon = 78$. We have calculated the population of different conformation using Maxwell−Boltzmann's statistics, and the result with $\epsilon = 5$ is in agreement with NMR results.

For these charged and flexible molecules, it is obvious that others methods may have to be used to get by MD study, more reasonable statistical participation of every structures to improve the NMR result. To simulate the molecular movements in solution, different protocols of Molecular Dynamics have been used, with the Biosym software INSIGHTII and DISCOVER.

Molecular Dynamics. For an exploration of the conformational space, after an equilibration period of 4 ps, the dynamics are run at 300 K with periodical jumps to 600 K to supply the system with energy (to pass conformational barriers). During a simulation a number of quantities, such as the potential and kinetic energies, are generally monitored to obtain a picture of the stability of the simulation.[26] The

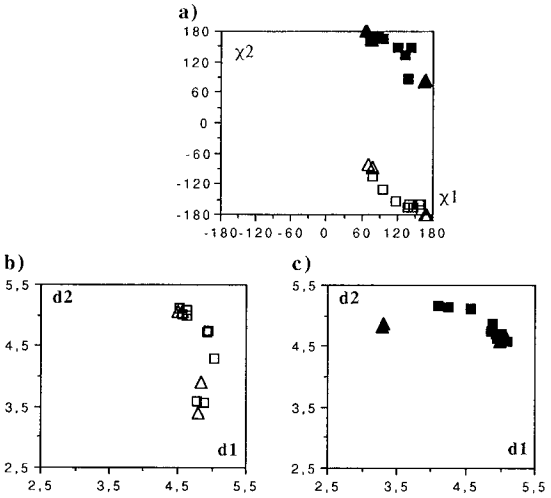

Figure 8. The different families for all the analogue conformations are represented in a diagram according to the physical features of the potentially active functional groups: (a) the repartition of alkyl chain torsion angles $\chi 1$ [C(1)−C(2)] and $\chi 2$[C(2)−C(3)]; (b) the three-dimensional interatomic distances between involved atoms, $d_{1(\alpha\text{-NH-}\gamma\text{-}CO_2^-)}$ and $d_{2(\alpha\text{-CO-}\gamma\text{-}CO_2^-)}$, for the *cis*-isomers; and (c) for the *trans*-isomers. (△) Boc-cis-C6-OMe, (□) Boc-cis-C5-OMe; (▲) Boc-trans-C6-OMe and (■) Boc-trans-C5-OMe.

50 ps trajectory is sampled every picosecond, the structures are then minimized by molecular mechanics and stored. The stability of the different conformers of BOC-*cis*- and -*trans*-C6 and -C5 has been tested by a 100 ps dynamics protocol at 300 K. We have run experiments starting from each one of the possible conformations of the four compounds to compare their energies and to determine their frequency in the interconversion. The results are summarized in Figures 4−6 and in Tables 3−5.

The amide bond between BOC and cyclohexane or cyclopentane fragment was fixed in the *trans* geometry, but the side chain around (ϕ) and (ψ) respectively CO(8)−C(1)−NH−CO(10) and O−CO(8)−C(1)−NH (Figure 2) is flexible and gives slight fluctuation to the total energy corresponding to its different conformations. The structures corresponding to (ϕ) dihedral angle values of either −60° or +60° which imply (ψ) dihedral angle values of ±50° or ±90° was stabler than that having (ϕ) or (ψ) ±170°. We conclude that our dataset is sufficient to define essentially folded (±60°) N-BOC conformational families. This is consistent with a type α-right or α-left helix which permits the ester chain to explore a large conformational space. It is interesting to notice that an extended structure (±170°) is required in the intermediate "higher-energy" structures when an interconversion is observed between the two chair conformations.

At each protocol, the energies and the calculated coupling constants from the different BOC-*cis*-C6-OMe **6** C1 and C2 conformers were compared (Table 3). In all the cases, the form C1 is obtained in agreement with the **6** solution and with an energy minimized smaller (3−7 kcal mol^{-1}) than that of the C2 conformer. The equilibrium is governed by a number of factors including the conformational free energy contributions of the individual substituents, as well as complex interactions between the substituents. These interactions are particularly marked in the C2 conformation which brings the two carboxy groups close to each other, namely in the diaxial *cis*-1,3 isomers [Figure 4a]. We have run dynamics, starting from each of these two conformers. At all the dynamic experiments considered, no interconversion has been observed until 600 K. It seems that there is a high energetic barrier between the two conformers. While the energy barrier separating the two chairs is usually in the range 10−12 kcal mol^{-1}, the difference in the free energy of the two conformers varies with the substituent: only at 800−1000 K with $\epsilon = 5$, an interconversion was observed and the **6 C2** (32.1 kcal mol^{-1}) conformer leads to the more stable conformer **6 C1** (29.7 kcal mol^{-1}) *via* a twist intermediate with energy about 4.8 kcal mol^{-1} above the minimum of the C2 conformer. Conversely, the **6 C1** structures are stable during the beginning of this protocol, but the experiment aborts with the rupture of the molecule, when the **6 C1** conformer leads to a twist-boat molecule with an energy minimized 10 kcal mol^{-1} above the minimum of the solution conformer **6 C1**.

For the BOC-*trans*-C6-OMe **7**, the *chair*−*chair* energy difference of 1 kcal mol^{-1} corresponding at 290 K to isomeric composition of 85/15 (experimental NMR data) is the balanced result of the influence of both substituents. We have run molecular mechanics calculations from each of the two conformers (**7 C1** and **7 C2**), to obtain NMR results. Correct energy difference (+0.7 kcal mol^{-1}) between the C1 and C2 forms are obtained for $\epsilon = 5$. We have run dynamics, starting from each of these two conformers. At all the dynamic experiments considered, the C1 and C2 conformers are stable, the energy of the C2 conformer is lower, and no interconversion has been observed until 1000 K. It seems that there is a high energetic barrier between the two conformers and only, at 1000 K with $\epsilon = 5$, an interconversion is observed. The **7 C1** (31.9 kcal mol^{-1}) conformer leads to the more stable conformer **7 C2** (29.3 kcal mol^{-1}) *via* a boat conformation (40.7 kcal mol^{-1}) and many twist-boat intermediates (40.6−41.8 kcal mol^{-1}) with energy about 10 kcal mol^{-1} higher than those of C1 conformer. However the experiments could not be achieved at this temperature. The **7 C2** structures are stable during all the protocol.

We have run dynamics from BOC-*cis*-C5-OMe **8** with explicit water molecules. The lowest-energy conformers E_1, ^2E, and E_3 were stable, confirming the results obtained with a protocol using $\epsilon = 5$. The γ-carboxylate group and the α-ester always adopted an equatorial (or isoclinal) position, whatever the conformation was. The less stable envelope conformers led to a more stable one *via* a twist intermediate, and interconversion was observed. The lowest energies structures achieved by MD (Figure 5, Table 4) are in good agreement with the NMR results (Table 2) according to E_5 or E_1, with γ-CO_2^- isoclinal and α-CO_2Me isoclinal or equatorial, and E_3, ^4E, or ^2E, with γ-CO_2^- equatorial and α-CO_2Me isoclinal or equatorial. The structures ^1E (α-CO_2Me axial and γ-CO_2^- isoclinal) represent the conformations with an higher same range energy and not in accordance with the NMR data.

In one type of structures BOC-*trans*-C5-OMe **9** generated by MD, the three functional groups (BOC-NH, α-CO_2Me, γ-CO_2^-) are equatorial-isoclinal (E_4, ^3E) and in the others structures two functional groups occupy two equatorial (E_2), two equatorial-isoclinal (^1E, ^5E), and two isoclinal (E_3) positions. The structures achieved by MD (Figure 6, Table 5) are in good agreement with NMR results (Table 2) according to γ-CO_2^- isoclinal, α-CO_2Me axial or equatorial, ^1E or ^5E, and γ-CO_2^- equatorial, α-CO_2Me axial or isoclinal, E_2 or E_4, ^3E. The structure E_3 (α-CO_2Me isoclinal and

γ-CO_2^- equatorial, α-CO_2Me axial or isoclinal, E_2 or E_4, ^3E. The structure E_3 (α-CO_2Me isoclinal and γ-CO_2^- axial) represents the structure of higher energy, and in this molecule $^3J_{H3C1}$ and $^3J_{H3C5}$ are not in agreement with the NMR data.

Structural Characteristics of These Inhibitors. The results from Table 1 show that all of the cycloderivatives N-BOC-α-monoesters **6**−**9** do not behave as substrates for the vitamin K-dependent carboxylase (Table 1). From the four cyclo-derivatives **6**−**9**, only *trans*-isomers (**7** and **9**) were much stronger inhibitors of BOC-Glu-OMe carboxylation than were *cis*-N-BOC-α-monoesters (**6** and **8**), although the efficiency of inhibition was very low. From the four compounds **6**−**9** tested, BOC-*trans*-C5-OMe (K_i = 20 mM) seems to be a better inhibitor than the other derivatives (K_i > 40 mM). Thus, its particular conformation compared to those of the derivatives without activity can give us information about the Glu side-chain conformation in the inhibitor carboxylase complex.

One conformation satisfying the conformational NMR study and energetical stability criterions was generated for BOC-*cis*-C6-OMe **6** and two for BOC-*trans*-C6-OMe **7** (Figure 4), but five different envelope for BOC-*cis*-C5-OMe **8** and BOC-*trans*-C5-OMe **9** (Figures 5 and 6).

The superimposition of C(1) and of the central atoms of the two functional groups (see numbering in Figure 2), *i.e.*, the α-N and α-C(8) of the different conformers deduced from the NMR and MD data of the four isomers analogues BOC-*cis*- and -*trans*-C6 and -C5 (Figure 7) displays conformational similarities. Analysis of structures generated by MD simulations for the four ligands were mostly similar, even though some superimpositional discrepancies occurred along BOC-NH-C(1)H-CO bonds. The main changes occur in the opposite direction of the chain and affect only the turn of the loop. An extended chain is found only in "high-energy" intermediate structures. The conformational energy and the electrostatic energy term were generally the most significant classification criterion from a physical point of view and allow to classify. More instructive is the comparison between the *cis*- and the *trans*-structures in terms of dihedral angles $\chi 1$ [α-CO−C(1)−C(2)−C(3)] and $\chi 2$ [C(1)−C(2)−C(3)−γ−CO_2^-] [Figure 8a].

The molecular modeling calculations on the *trans*-isomer indicate that the most stable conformation is one in which the molecule has torsion angles $\chi 1$ of about 60−120° and $\chi 2$ of approximately 180°, whereas for the *cis*-isomers the very extended $\chi 1 = 180°$ and $\chi 2 = 180°$ are respectively 100% populated. The calculations have included the hydration effects of the aqueous solvent. Rather than classify the conformational populations by combinations of $\chi 1$ and $\chi 2$, they are grouped in a second step according to the distance (d_1) between the N atom and the carbon atom of the γ-CO_2^- group, but pairs with the same N−γCO_2^- distance will differ in the distance between carboxy groups (d_2) [Figure 8 (parts b and c)]. Two groups are considered in electrostatic interaction if their distance is less (or equal) than 4 Å.

The results represent two groups of structures whose dihedral angles and distances (d_1) and (d_2) suggested that they may belong to the same conformational family, in order to keep a limited number of classes (**I**−**IV**). Two families are characterized by the d_1 (α-NH−γ-CO_2^-) distance less than the d_2 (α-CO−γ-CO_2^-) one: **I** ($d_1 \ll d_2$) and **II** ($d_1 < d_2$). Conversely, two others families are characterized by the d_2 distance less than the d_1 one: **IV** ($d_2 \ll d_1$) and **III** ($d_2 < d_1$). For the inactive BOC-*cis*-C6-OMe **6**, the distances d_1 = 4.5 Å and d_2 = 5.1 Å correspond in this case to a standard type **II** family [Figure 8b], while different values for the predominant BOC-*trans*-C6-OMe **7** isomer, d_1 = 5.1 Å and d_2 = 4.6 Å correspond to the **III** family [Figure 8c]. For this compound, the NMR data shows that the major conformer is in equilibrium with a minor one characterized by the distances d_1 = 3.3 Å and d_2 = 4.8 Å and belonging to the **I** family [Figure 8c]. The classification of the modeled cyclopentane analogues leads to three classes of low energy conformations which include more than 80% of the total number of structures. Figures 7(c),(d) represent these three classes for the BOC-*cis*-C5-OMe **8** (families **II**, **III**, and **IV**) and for the better inhibitor BOC-*trans*-C5-OMe **9** (families **I**, **II**, and **III**). Some conclusions can also be drawn for BOC-*cis*-C5-OMe **8** and BOC-*trans*-C5-OMe **9** (Figure 3). Class **II** [Figure 3a] containing E_1, ^2E, and E_3 with the more extended carboxy groups (α-CO_2Me and γ-CO_2^-) for BOC-*cis*-C5-OMe **8** and class **III** [Figure 3b] containing structures with the two 1,4 functional (α-NH-BOC and γ-CO_2^-) groups equatorial-isoclinal E_2, ^1E, and ^3E for BOC-*trans*-C5-OMe **9** are the most populated stable conformers. The classes which are neglected in the analysis individually represent less than 4% of the total number of structures.

CONCLUSION

The modeled structures generated for the four glutamic acid analogues appear to be very stable, in accordance with NMR data. They exhibit different conformations, more or less extended. The structures have been successfully classified into a reduced number of homogeneous classes, according to their internal electrostatic and essentially steric interactions. Two conformational collections are respectively observable for *cis* and *trans* isomers (Figure 8).

These molecules are inhibitors for the vitamin K-dependent carboxylation and they were very different in their reaction with the carboxylase. Since the BOC-*trans*-C5-OMe **9** exhibits a strong biological activity, while the BOC-*cis*-C6-OMe **6** is the worse biological active then their classification gives an insight into the structure−activity relationship. Since one stable class **III** of conformations is particular to the biologically active BOC-*trans*-C5-OMe **9**, while it is not accessible to the nonactive BOC-*cis*-C6-OMe **6**, a development of the current work should go in this direction. The nonactive **6** belongs to the class **II** family which exhibits the more "extended" carboxy groups (α-CO_2Me and γ-CO_2^-) conformation.

The molecular flexibility of the *trans*-isomers is important, and it is probably interesting that substrate molecules possess some flexibility to be able to respond to the perturbations presented by the active site during their mutual interaction.

ACKNOWLEDGMENT

This Work was supported by grants from the DIAGNOSTICA STAGO-GEHT (Groupes d'études sur l'Hémostase et la Thrombose).

REFERENCES AND NOTES

(1) Suttie, J. W. Vitamin K-dependent Carboxylase. *Ann. Rev. Biochem.* **1985**, *54*, 459−477.
(2) Vermeer, C.; De Boer-Van den Berg, M. A. G. Vitamin K-dependent carboxylase. *Haematologia* **1984**, *18*, 71−97.

(3) Furie, B.; Furie, B. C. The molecular basis of blood coagulation. *Cell*. **1988**, *53*, 505−518.
(4) Suttie, J. W. In *Handbook of Vitamins*, 2nd ed.; Machlin, L. J., Ed.; Marcel Dekker, Inc.: New York, 1991; pp 145−194.
(5) Finna, J. H.; Goodman, L.; Suttie, J. W. In *Vitamin K Metabolism and Vitamin K Dependent Proteins*; Suttie, J. W., Ed.; University Park Press: Baltimore, 1980; pp 480−483.
(6) Rich, D. H.; Leehrman, S. R.; Kawai, M.; Goodman, H. L.; Suttie, J. W. In *Vitamin K Metabolism and Vitamin K dependent Proteins*; Suttie, J. W., Ed.; University Park Press: Baltimore, 1980; pp 471−479.
(7) Decottignies-Le Marechal, P.; Ducrocq, C.; Marquet, A.; Azerad, R. The stereochemistry of hydrogen abstraction in vitamin K-dependent carboxylation. *J. Biol. Chem.* **1984**, *259*, 15010−15012.
(8) Azerad, R.; Decottignies-Le Marechal, P.; Ducrocq, C.; Righini-Tapie, A.; Vidal-Cros, A.; Bory, S.; Dubois, J.; Gaudry, M.; Marquet, A. *Current Advances in Vitamin K Research*; Suttie, J. W., Ed.; Elsevier: New York, 1988; pp 17−24.
(9) Soute, B. A. M.; Acher, F.; Azerad, R.; Vermeer, C. Vitamin K-dependent carboxylase: effect of ammonium sulfate on substrate carboxylation and on inhibition by stereospecific substrate analogs. *Biochim. Biophys. Acta* **1990**, *1034*, 11−16.
(10) Dubois, J.; Gaudry, M.; Bory, S.; Azerad, R.; Marquet, A. Vitamin-K Dependent Carboxylation. Study of the hydrogen abstraction stereochemistry wity γ-fluoroglutamic acid-containing peptides. *J. Biol. Chem.* **1983**, *264*, 14145−14150.
(11) Ducrocq, C.; Righini-Tapie, A.; Azerad, R.; Green, J. F.; Friedman, P. A.; Beaucourt, J. P.; Rousseau, B. Synthesis of L-glutamic acid stereospecifically labelled at C-4 with tritium: Stereochemistry of tritium release catalyzed by the Vitamin K-dependent carboxylase in the absence of carboxylation. *J. Chem. Soc., Perkin Trans. 1* **1986**, 1323−1328.
(12) Dubois, J.; Dugave, C.; Foures, C.; Kaminsky, M.; Tabet, J. C.; Bory, S.; Gaudry, M.; Marquet, A. Vitamin-K Dependent Carboxylation - Determination of the Stereochemical Course Using 4-Fluoroglutamyl-Containing Substrate. *Biochemistry* **1991**, *30*, 10506−10512.
(13) Acher, F.; Azerad, R. Synthesis of Diastereoisomeric Peptides Incorporating Cycloglutamic Acids - Substrate Specificity of Vitamin K-Dependent Carboxylation. *Int. J. Peptide Protein Res.* **1991**, *37*, 210−219.
(14) Bucourt, R. In *Topics in Stereochemistry*; Eliel, E. L., Allinger, N. L., Eds.; Wiley: New York, 1974; pp 159−224.
(15) Testa, B. In *Principles of Organic Stereochemistry*; Dekker: New York, 1979; pp 112−113.
(16) Cremer, D. A general definition of ring substituent positions. *Isr. J. Chem.* **1980**, *20*, 12−19.
(17) Fuchs, B. *Topics in Stereochemistry*; Eliel, E. L., Allinger, N. L.; Wiley: New York, **1978**, *10*, 1−94.
(18) Altona, C.; Sundaralingam, M. Conformational Analysis of the Sugar Ring in Nucleosides and Nucleotides. Improved Metodes for the Interpretation of Proton Magnetic Resonance Coupling Cosntants. *J. Am. Chem. Soc.* **1973**, *95*, 2333−2344.
(19) Haasnoot, C. A. G.; de Leeuw, F. A. A. M.; Altona, C. The relation between proton−proton NMR coupling constants and substituent electronegativities. I. An empirical generalization of the Karplus equation. *Tetrahedron* **1980**, *36*, 2783−2792.
(20) Tvaroska, I.; Hricovini, M.; Petrakova, E. An attempt to derive a new Karplus-type equation of vicinal proton-carbon coupling constants for C−O−C−H segments of bonded atoms. *Carbohydr. Res.* **1989**, *189*, 359−362.
(21) Ladam, P.; Gharbi-Benarous, J.; Pioto, M.; Delaforge, M.; Girault, J. P. Determination of Long-Range 13C-1H Coupling Constants of Macrolide Antibiotics by 2D J-δ Selective INEPT experiments. *Magn. Reson. Chem.* **1994**, *32*, 1−7.
(22) Morelle, N.; Gharbi-Benarous, J.; Acher, F.; Valle, G.; Crisma, M.; Toniolo, C.; Azerad, R.; Girault, J. P. Conformational Analysis of Cyclohexane-derived Analogues of Glutamic Acid by X-Ray Cristallography, NMR Spectroscopy in Solution, and Molecular Dynamics. *J. Chem. Soc., Perkin Trans. 2* **1993**, 525−.
(23) Larue, V.; Gharbi-Benarous, J.; Acher, F.; Valle, G.; Crisma, M.; Toniolo, C.; Azerad, R.; Girault, J. P. Conformational Analysis by NMR Spectroscopy, Molecular Dynamics Simulation in Water and X-Ray Crystallography of Glutamic Acid Analogues: Isomers of 1-Amino-1,3-Cyclopentane Dicarboxylic Acid (ACPD). *J. Chem. Soc., Perkin Trans. 2* **1995**, 1111−1126.
(24) Dauber-Osguthorpe, P.; Roberts, V. A.; Osguthorpe, D. J.; Wolff, J.; Genest, M.; Hagler, A. T. Structure and Energetics of Ligand Binding to Proteins: E. coli Dihydrofolate Reductase-Trimethoprim, A Drug-Receptor System. *Proteins: Structure, Function Genetics* **1988**, *4*, 31−47.
(25) Burt, S. K.; Mackay, D.; Nagler, A. T. In *Computer-Aided Drug Design*; Perun, T. J., Propst, C. L., Eds.; Marcel Dekker: New York and Basel, 1989; p 66.
(26) van Gunsteren, W. F.; Berendsen, H. J. C. Computer Simulation of Molecular Dynamics: Methodology, Applications, and Perspectives in Chemistry. *Angew. Chem., Int. Ed. Engl.* **1990**, *29*, 992−1023.

CI950153J